

This article was downloaded by: [University of Hong Kong]

On: 24 April 2010

Access details: Access Details: [subscription number 916418249]

Publisher Taylor & Francis

Informa Ltd Registered in England and Wales Registered Number: 1072954 Registered office: Mortimer House, 37-41 Mortimer Street, London W1T 3JH, UK



Hydrological Sciences Journal

Publication details, including instructions for authors and subscription information:

<http://www.informaworld.com/smpp/title~content=t911751996>

Theoretical study of the impact of tide-induced airflow on hydraulic head in air-confined coastal aquifers

Haipeng Guo ^{ab}; Jiu J. Jiao ^a

^a Department of Earth Sciences, The University of Hong Kong, Hong Kong, China ^b China Institute of Geo-Environment Monitoring, Beijing, China

Online publication date: 23 April 2010

To cite this Article Guo, Haipeng and Jiao, Jiu J. (2010) 'Theoretical study of the impact of tide-induced airflow on hydraulic head in air-confined coastal aquifers', *Hydrological Sciences Journal*, 55: 3, 435 – 445

To link to this Article: DOI: 10.1080/02626661003739959

URL: <http://dx.doi.org/10.1080/02626661003739959>

PLEASE SCROLL DOWN FOR ARTICLE

Full terms and conditions of use: <http://www.informaworld.com/terms-and-conditions-of-access.pdf>

This article may be used for research, teaching and private study purposes. Any substantial or systematic reproduction, re-distribution, re-selling, loan or sub-licensing, systematic supply or distribution in any form to anyone is expressly forbidden.

The publisher does not give any warranty express or implied or make any representation that the contents will be complete or accurate or up to date. The accuracy of any instructions, formulae and drug doses should be independently verified with primary sources. The publisher shall not be liable for any loss, actions, claims, proceedings, demand or costs or damages whatsoever or howsoever caused arising directly or indirectly in connection with or arising out of the use of this material.

Theoretical study of the impact of tide-induced airflow on hydraulic head in air-confined coastal aquifers

Haipeng Guo^{1,2} & Jiu J. Jiao¹

¹Department of Earth Sciences, The University of Hong Kong, Hong Kong, China
hpguo79@gmail.com; jjiao@hku.hk

²China Institute of Geo-Environment Monitoring, Beijing 100081, China

Received 16 January 2009; accepted 21 September 2009; open for discussion until 1 October 2010

Citation Guo, H.-P. & Jiao, J. J. (2010) Theoretical study of the impact of tide-induced airflow on hydraulic head in air-confined coastal aquifers. *Hydrol. Sci. J.* 55(3), 435–445.

Abstract Tide-induced hydraulic head fluctuation results in significant airflow above the water table if the aquifer is air-confined, for example, if the aquifer is capped by low permeability materials. Hypothetical studies on the interaction between tidal fluctuation and airflow in coastal aquifers are carried out using an air–water two-phase numerical model. The results show that both the amplitude of the hydraulic head fluctuation and the distance of influence of the tidal fluctuation increase due to the impact of airflow. For a fixed distance from the coastline, the amplitude of the hydraulic head fluctuation increases with depth, and the hydraulic head fluctuation at small depths lags that at great depths. Tide-induced airflow may be so strong that considerable errors in estimating hydraulic parameters could be generated when models are applied without considering airflow. In an air-confined aquifer, if airflow is neglected, the hydraulic diffusivity could be considerably overestimated.

Key words hydraulic head fluctuation; tidal fluctuation; air-confined aquifer; hydraulic parameters; hydraulic diffusivity

Etude théorique de l'impact de la circulation de l'air due à la marée sur le potentiel hydraulique des aquifères côtiers à nappe captive

Résumé La fluctuation du potentiel hydraulique due à la marée engendre une circulation d'air significative au-dessus de la nappe d'eau si l'aquifère est à nappe captive, par exemple si l'aquifère est surmonté de matériaux à faible perméabilité. Des études hypothétiques sur l'interaction entre fluctuation due à la marée et circulation d'air dans les aquifères côtiers sont conduites à l'aide d'un modèle numérique biphasique air–eau. Les résultats montrent que l'amplitude de fluctuation du potentiel hydraulique et la distance d'influence de la fluctuation due à la marée augmentent toutes les deux à cause de l'impact de la circulation d'air. Pour une distance à la côte fixée, l'amplitude de fluctuation du potentiel hydraulique augmente avec la profondeur, et la fluctuation du potentiel hydraulique à de petites profondeurs est en retard sur celle à de grandes profondeurs. La circulation d'air due à la marée peut être si forte que de considérables erreurs d'estimation des paramètres hydrauliques peuvent être générées quand on applique des modèles sans tenir compte de la circulation de l'air. Dans un aquifère à nappe captive, si la circulation d'air est négligée, la diffusivité hydraulique peut être considérablement sous-estimée.

Mots clefs fluctuation du potentiel hydraulique; fluctuation due à la marée; aquifère à nappe captive; paramètres hydrauliques; diffusivité hydraulique

INTRODUCTION

Social and economic development in coastal areas has caused various environmental and engineering problems such as seawater intrusion, beach dewatering, pollution of coastal aquifers, and stability of coastal structures (Carr, 1969; Pontin, 1986; Chan & Mohsen, 1992; Li *et al.*, 1996; Jiao & Tang, 1999). Most of these problems are related to the dynamic interaction between groundwater and seawater, which has been well studied since 1950s. With the rapid development

of computer techniques, numerical methods have been widely adopted to investigate the interaction between seawater and groundwater in coastal areas (e.g. Pandit *et al.*, 1991; Robinson & Gallagher, 1999; Ataie-Ashtiani *et al.*, 2001). In most of these existing studies, the airflow in the unsaturated zone is neglected, i.e. the gas phase is treated as a passive bystander at constant pressure. In some cases, however, the airflow may be very significant so that it cannot be ignored (Jiao & Li, 2004; Guo & Jiao, 2008). Heaving of the airfield

pavement at the Hong Kong International Airport was observed which caused by the abnormally high air pressure below the pavement due to a combined tidal and wet weather effect. The heave problem was solved by installing vertical deep-ventilation pipes to release the air pressure (Leung *et al.*, 2007).

Although subsurface airflow has been investigated in some laboratory or field conditions (e.g. Shan, 1995; Elberling *et al.*, 1998; Weeks, 2002; Guo *et al.*, 2008), the impact of airflow on hydraulic head fluctuation has not been well addressed in the literature. Jiao & Li (2004) employed a two-dimensional numerical model to investigate relations among sea tides, groundwater in the aquifer, airflow in the unsaturated zone, barometric pressure variations, and rainfall in a coastal reclamation site. Their simulation results revealed that significantly high and low subsoil air pressures could be generated when different conditions, such as rainfall, stratum structure and tidal fluctuations combined favourably. Li & Jiao (2005) developed an analytical solution to investigate vertical airflow driven by a periodically fluctuating water table in a coastal two-layered system. In the model by Jiao & Li (2004), it was assumed that the water table fluctuated at the same frequency and amplitude as the sea tide due to the high permeability of the aquifer. This assumption may be unreasonable in coastal areas of typical permeabilities. Guo & Jiao (2008) conducted a numerical study of tide-induced airflow in unsaturated zones in a coastal two-layered subsurface system using more realistic boundary assumptions. They concluded that significant air flow could be induced in air-confined aquifers, i.e. the permeability of the upper layer is at least two orders of magnitude smaller than that of the lower layer, and that strong relations existed between fluctuations of the air pressure and the water level.

Tide-induced groundwater fluctuation can result in significant airflow in the unsaturated zone (Guo & Jiao, 2008), which may in turn impact hydraulic head fluctuations in the aquifer. However, this phenomenon was studied only recently and coastal hydrogeologists may still fail to understand the process. The aim of this paper is to investigate the effect of the airflow on water level calculation and aquifer parameter estimation if the airflow is ignored.

The simulator TOUGH2 was used to obtain numerical solutions of the air–water two-phase model for different cases. A similar model setup and boundary conditions to those used by Guo &

Jiao (2008) were employed for the numerical simulations. Comparisons were made among the hydraulic head fluctuations in an air-unconfined aquifer without airflow, air-confined aquifers and a water-confined aquifer. The tide-induced airflow may impact the water level fluctuation in the aquifer so much that the aquifer hydraulic parameters may be incorrectly estimated with models in which airflow is neglected. The possible parameter estimation errors when airflow is ignored are analysed in detail.

NUMERICAL MODEL

Domain description

Guo & Jiao (2008) investigated the tide-induced airflow in a two-layered, two-dimensional subsurface system (Fig. 1). Such a two-layered system is common along natural coasts near estuary areas and urbanized coasts where soils are covered by impermeable construction materials. Tide-induced airflow is significant only when the system is air-confined, i.e. the permeability of the upper layer is much less than that of the lower layer (Guo & Jiao, 2008). Otherwise, the system is air-unconfined and the airflow or air pressure can be ignored. If the bottom of the upper layer is below the water level and the permeability of the upper layer is less than that of the lower layer, the system becomes a traditional water-confined aquifer.

The model setup and boundary conditions in this study are similar to those used by Guo & Jiao (2008). The interface between the two layers is at a depth of 3.3 m below the ground surface. The right boundary is set to be 1000 m from the coastline and represented by a no-flow boundary. This is reasonable in that usually no disturbance induced by sea tide can reach this distance. A no-flow boundary is also set at the base of the domain, which is 17.3 m below the ground surface. Without loss of generality, a single-component sinusoidal, diurnal tide is used as the tidal boundary. The tidal variation h_{tide} can be expressed as:

$$h_{\text{tide}} = -h_{\text{msl}} + A \cos(\omega t + \varepsilon) \quad (1)$$

where h_{msl} is the mean sea level, and A , ω and ε are the amplitude, radian frequency and radian phase shift, respectively, of the tidal fluctuation. The following parameter values were used to determine the tidal variation: $h_{\text{msl}} = 6.05$ m; $A = 1.25$ m; $\omega = 2\pi$ d⁻¹; and $\varepsilon = 1.6$.

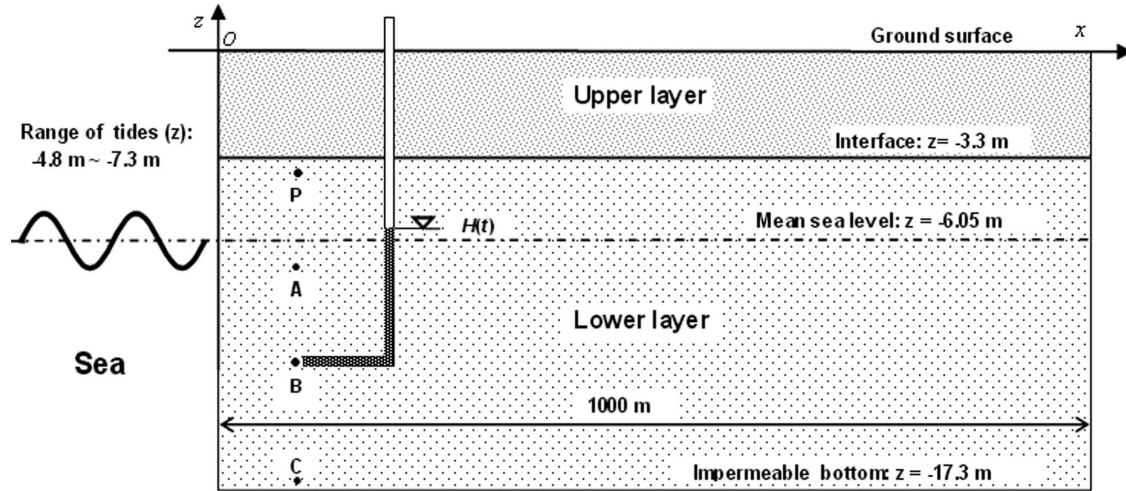


Fig. 1 Sketch of a coastal two-layered subsurface system (after Guo & Jiao, 2008) ($z = 0$ m at the ground surface, $z < 0$ m downward; $x = 0$ m at the coastline, $x > 0$ m landward).

In areas close to the coastline, the barometric pressure may have a less important impact on subsurface airflow than tide-induced water level fluctuations because the frequency and amplitude of the barometric pressure fluctuation are usually much smaller than those of the sea tides (Jiao & Li, 2004; Guo & Jiao, 2008). In the numerical simulation, the time-independent Dirichlet boundary condition with a fixed pressure of 101.3 kPa is applied on the upper boundary and the left boundary above the sea level to represent the atmospheric boundary.

Governing equations

The mathematical model describing two-phase air-water flow is based on the mass conservation equations. The mass balance equation under isothermal condition can be written in the following form (Pruess *et al.*, 1999):

$$\frac{d}{dt} \int_{V_n} M^\kappa dV_n = \int_{\Gamma_n} \mathbf{F}^\kappa \cdot \mathbf{n} d\Gamma_n + \int_{V_n} q^\kappa dV_n \quad (2)$$

The integration is over an arbitrary sub-domain, V_n , of the flow system under study, which is bounded by a closed surface, Γ_n . The quantity M appearing in the accumulation term (left-hand side) represents mass per volume, with κ denoting the mass component of air or water. The term \mathbf{F} denotes mass flux, q denotes sinks and sources, \mathbf{n} is a unit normal vector on surface element $d\Gamma_n$, pointing inward into V_n .

The general form of the mass accumulation term in equation (2) can be written as:

$$M^\kappa = \phi \sum_{\beta} S_{\beta} \rho_{\beta} X_{\beta}^{\kappa} \quad (3)$$

The total mass of component κ (air or water) is obtained by summing over the fluid phases β (liquid or gas); ϕ is porosity, S_{β} is the saturation of phase β (i.e. the fraction of pore volume occupied by phase β), ρ_{β} is the density of phase β , and X_{β}^{κ} is the mass fraction of component κ present in phase β .

The advective mass flux of a component (air or water) is a sum over phases. It can be written as:

$$\mathbf{F}^\kappa = \sum_{\beta} X_{\beta}^{\kappa} \mathbf{F}_{\beta} \quad (4)$$

Individual phase fluxes are given by a multiphase version of Darcy's law:

$$\mathbf{F}_{\beta} = \rho_{\beta} \mathbf{u}_{\beta} = -k \frac{k_{r\beta} \rho_{\beta}}{\mu_{\beta}} (\nabla P_{\beta} - \rho_{\beta} \mathbf{g}) \quad (5)$$

here \mathbf{u}_{β} is the Darcy velocity (volume flux) in phase β ; k is absolute permeability; $k_{r\beta}$ is relative permeability to phase β ; μ_{β} is viscosity; P_{β} is the fluid pressure in phase β ; and \mathbf{g} is the vector of gravitational acceleration. The pressures in liquid phase (P_l) and gas phase (P_g) are related via the capillary pressure, P_{cap} :

$$P_l = P_g + P_{\text{cap}} \quad (6)$$

Soil parameters used in the numerical simulation

The permeabilities of the upper and lower layers are represented as k_U and k_L , respectively. The permeabilities of both the two layers are assumed to be homogeneous and isotropic. Five well-studied soil types covering a typical range of representative permeability conditions are used in this paper. The soil parameters of these soil types are statistics of the analysis results of a soil database compiled by Carsel *et al.* (1988). In order to systematically examine the impact of the permeability on the relation between the hydraulic head and airflow, a wider range of permeability values need to be considered. For this purpose, a new soil is designed for the upper layer based on a silty clay. The absolute permeability of this soil is set to be 10^{-16} m² and all the other parameters remain the same as those of silt clay. This designed soil is not unrealistic since the coefficient of variation of the hydraulic conductivity for silt clay is as great as 453.3% (Carsel & Parrish, 1988, Table 4). Table 1 lists the absolute permeability k and soil parameters including porosity ϕ , the saturated and residual water saturation S_{ls} and S_{lr} , and the van Genuchten water retention parameters, n and α , for these soil types.

In the simulations, the van Genuchten function (van Genuchten, 1980) is used to describe the capillary pressure, P_{cap} :

$$P_{cap} = -\frac{\rho_w g}{\alpha} ([S^*]^{-\frac{n}{n-1}} - 1)^{\frac{1}{n}} (-P_{max} \leq P_{cap} \leq 0) \quad (7)$$

where $S^* = (S_l - S_{lr}) / (S_{ls} - S_{lr})$, S_l is water saturation, ρ_w is density of water, g is the gravitational constant, and α and n are fitting parameters.

The van Genuchten-Mualem model (Mualem, 1976; van Genuchten, 1980) is used to simulate the liquid relative permeability, k_{rl} :

$$k_{rl} = \begin{cases} \sqrt{S^*} \left\{ 1 - (1 - [S^*]^{-\frac{n}{n-1}})^{\frac{n-1}{n}} \right\}^2 & (S_l < S_{ls}) \\ 1 & (S_l \geq S_{ls}) \end{cases} \quad (8)$$

The gas relative permeability, k_{rg} , is chosen as one of the following two forms, the second of which is due to Corey (1954) (Pruess *et al.*, 1999):

$$k_{rg} = \begin{cases} 1 - k_{rl} & (S_{gr} = 0) \\ (1 - \hat{S})^2 (1 - \hat{S}^2) & (S_{gr} > 0) \end{cases} \quad (9)$$

with $\hat{S} = (S_l - S_{lr}) / (1 - S_{lr} - S_{gr})$ and S_{gr} is residual gas saturation.

Numerical method

The TOUGH2 code (Pruess *et al.*, 1999), a numerical simulator for flows of multicomponent, multiphase fluids in multi-dimensional porous and fractured media, is used to obtain the numerical solutions of the mathematical model. The TOUGH2 code includes ten different EOS (equation-of-state) modules, and various EOS modules can represent different fluid mixtures. In this paper, the EOS3 module is used to simulate the air-water two-phase flow problem under isothermal conditions (25°C). The air is treated as a compressible ideal gas in this study. A Cartesian mesh is used for the numerical simulations. The model domain is divided into 78 layers and 103 columns.

Four observation points at a distance of 23 m from the coastline are selected to discuss the simulation results (Fig. 1). Point P is in the unsaturated zone and at a depth of 4.2 m below the ground surface. Points A, B, and C are in the saturated zone and at depths of 7.7, 13 and 17.3 m below the ground surface, respectively.

NUMERICAL RESULTS AND DISCUSSION

The tide-induced hydraulic head fluctuation results in air pressure fluctuations in the unsaturated zone. Similarly, the air pressure fluctuations may in turn have some impact on the hydraulic head fluctuation. The primary objective of this section is to investigate how airflow in the unsaturated zone impacts the hydraulic head fluctuation in the aquifer.

Table 1 Primary parameter values used in the numerical simulation.

	Soil type	k (m ²)	ϕ (cm ³ /cm ³)	S_{ls} (cm ³ /cm ³)	S_{lr} (cm ³ /cm ³)	n	α (m ⁻¹)
Upper layer	Silty clay	5.06×10^{-15} 1.0×10^{-16}	0.399	0.902	0.175	1.09	0.5
	Silty clay loam	1.77×10^{-14}	0.48	0.896	0.185	1.23	1.0
	Silt loam	1.14×10^{-13}	0.486	0.926	0.138	1.41	2
	Sandy loam	1.12×10^{-12}	0.445	0.921	0.146	1.89	7.5
Lower layer	Sand	10^{-11}	0.454	0.947	0.099	2.68	14.5

Hydraulic head fluctuation in an air-unconfined aquifer compared with that in air-confined aquifers

In order to investigate the effects of the airflow in the unsaturated zone on the hydraulic head in the aquifer, comparisons are made between numerical solutions with and without airflow. The case without airflow is approximated using the following approach. The gas phase is treated as a passive bystander at constant pressure, and the numerical solution is approximately obtained using a very large gas permeability in the air–water two-phase model. The air pressure above the water table is almost a constant over time when the relative permeability of gas phase, k_{rg} , is multiplied by a factor of 200. In this case, the system is virtually air-unconfined.

Table 2 shows the simulation results with and without airflow in the unsaturated zone with $k_L = 10^{-11} \text{ m}^2$, where A_B is the calculated amplitude of the hydraulic head at point B (see Fig. 1 for the location) and A_{tide} is the tidal amplitude at the coastline. The influence distance is defined as the distance between the coastline and the observation point at which the amplitude of the hydraulic head is 1% of the tidal amplitude.

To compare the differences in amplitude and influence distance between the air-unconfined aquifer and air- or water-confined aquifer, two more parameters are introduced: amplitude ratio (R_a) and influence distance ratio (R_{id}). The former is defined as the ratio between the amplitude at Point B in the air- or water-confined aquifer and that in the air-unconfined aquifer, while the latter is defined as the ratio between the influence distance in the air- or water-confined aquifer and that in the air-unconfined aquifer. For example, R_a for the air-confined case with $k_U/k_L = 1.12 \times 10^{-1}$ is calculated as $0.12/0.11 = 1.09$ and R_{id} is calculated as $49.0/48.4 = 1.01$ (Table 2). Both the amplitude ratio, R_a , and influence distance ratio, R_{id} , are almost 1, indicating that the system with $k_U/k_L = 1.12 \times 10^{-1}$ is only slightly air-confined and there is not much

difference between the amplitude or influence distance in the air-unconfined and air-confined aquifers.

There is an obvious increase in both the amplitude at point B and the influence distance as the ratio of k_U/k_L decreases to 1.14×10^{-2} , in which case the aquifer is more air-confined. As k_U/k_L decreases to 10^{-5} , the amplitude at point B is increased to 0.32 m, which is 2.91 times greater than that without airflow. Also, the influence distance is increased to 203.9 m, which is 4.21 times greater than the influence distance without airflow.

The above discussion shows that airflow will have an impact on the water level fluctuation in the aquifer when the ratio k_U/k_L is small. The impact can be significant when k_U is over two orders smaller than k_L . This is because, if k_U is small, the resistance of the upper layer to the airflow is significant and it is difficult for the subsurface air to escape to the atmosphere when the water table rises. Similarly, the air in the atmosphere cannot easily flow into the subsurface soil as the water table falls. Thus, a large air pressure fluctuation above the water table may be induced. Figure 2 shows how the air pressure at the observation point P changes with time for different ratios of k_U/k_L when the permeability of the lower layer (k_L) is fixed at 10^{-11} m^2 . For $k_U/k_L = 5.06 \times 10^{-4}$, 1.77×10^{-3} , 1.14×10^{-2} and 1.12×10^{-1} , the corresponding amplitude of the air pressure fluctuation at point P is 2.04, 1.8, 0.95 and 0.11 kPa, respectively, which is 2.0, 1.8, 0.9 and 0.1% of the atmospheric pressure of 101.3 kPa. As k_U/k_L decreases, the airflow above the water table becomes more significant so that the groundwater is effectively under confined conditions and the head fluctuation dies out more slowly with distance.

Hydraulic head fluctuation in air-confined aquifers compared with that in a water-confined aquifer

A water-confined aquifer is simulated in order to compare tide-induced groundwater fluctuations in air- and water-confined aquifers. The bottom of the confining

Table 2 The amplitude, A_B , of the hydraulic head at point B, A_B/A_{tide} , amplitude ratio, R_a , influence distance, and influence distance ratio, R_{id} for different cases with $k_L = 10^{-11} \text{ m}^2$.

Case	$k_U \text{ (m}^2\text{)}$	k_U/k_L	$A_B \text{ (m)}$	$A_B/A_{\text{tide}} \text{ (\%)}$	R_a	Influence distance (m)	R_{id}
Air-unconfined aquifer	-	-	0.11	8.8	1.0	48.4	1.0
Air-confined aquifer	1.12×10^{-12}	1.12×10^{-1}	0.12	9.6	1.09	49.0	1.01
	1.14×10^{-13}	1.14×10^{-2}	0.18	14.4	1.64	87.6	1.81
	1.77×10^{-14}	1.77×10^{-3}	0.27	21.6	2.45	151.4	3.13
	5.06×10^{-15}	5.06×10^{-4}	0.29	23.2	2.64	173.8	3.59
	1.0×10^{-16}	1.0×10^{-5}	0.32	25.6	2.91	203.9	4.21
Water-confined aquifer	-	-	1.02	81.6	9.27	495.2	10.23

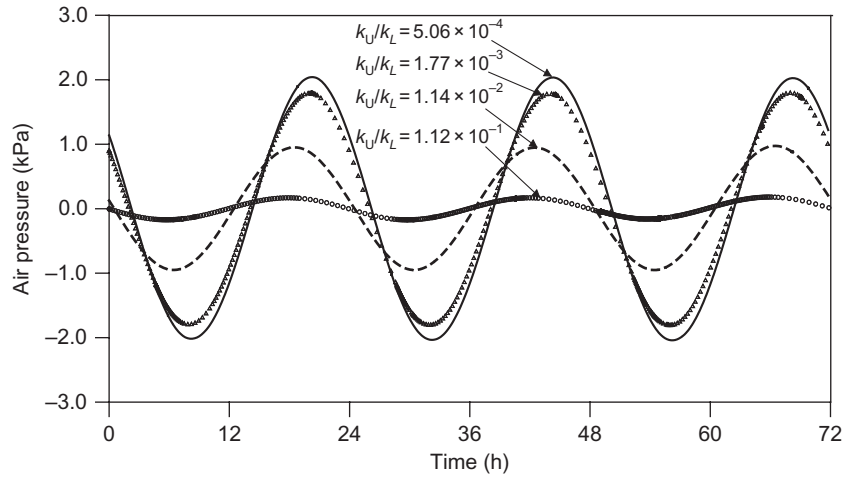


Fig. 2 Temporal changes of air pressure at point P for different ratios of k_U/k_L with $k_L = 10^{-11} \text{ m}^2$.

unit is extended from 2.75 m a.m.s.l. to 1.35 m below m.s.l. The hydraulic conductivity and specific storage of the confining unit are assumed to be 0.013 m/d and $2.5 \times 10^{-4} \text{ m}^{-1}$, respectively, which are based on parameters estimated from a field pumping test (Sheahan, 1977).

Figure 3 shows temporal changes of the hydraulic heads at point B in an air-unconfined aquifer without airflow, air-confined aquifers, and a water-confined aquifer when k_L is fixed at 10^{-11} m^2 . The water head fluctuation in air-unconfined and air-confined aquifers lags that in water-confined aquifers because the diffusivity of air-unconfined and air-confined aquifers is smaller than that of water-confined aquifers. It is clearly shown that the amplitude in the water-confined

aquifer is the greatest, and the amplitude in air-confined aquifers is greater than that in the air-unconfined aquifer without airflow.

As shown in the last row in Table 2, the calculated amplitude at point B in the water-confined aquifer is 1.02 m, about 82% of the tidal amplitude, and the influence distance is 495 m. The amplitude of the hydraulic head fluctuation and the influence distance are much greater than those of air-confined aquifers, even though the airflow is significant, indicating that a water-confining unit has a more significant impact on the hydraulic head than airflow in air-confined aquifers. However, the characteristics of the hydraulic head fluctuation in air-confined aquifers change greatly due to airflow above the water table compared with

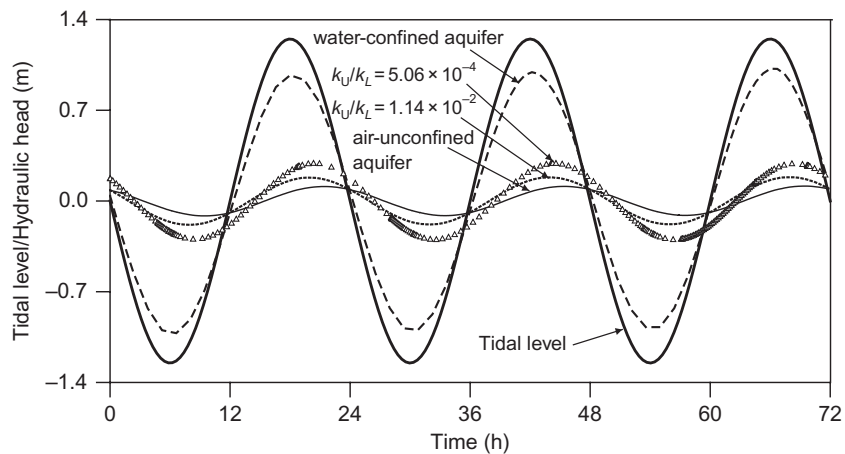


Fig. 3 Temporal changes of the hydraulic head at point B with $k_L = 10^{-11} \text{ m}^2$ in an air-unconfined aquifer without airflow (thin solid curve), air-confined aquifers with $k_U/k_L = 1.14 \times 10^{-2}$ (dotted curve) and $k_U/k_L = 5.06 \times 10^{-4}$ (triangles), and a water-confined aquifer (dashed curve).

Downloaded By: [University of Hong Kong] At: 02:39 24 April 2010

air-unconfined aquifers without airflow. The fluctuations of the hydraulic head in air-confined aquifers tend to be similar to certain degree to those in a water-confined aquifer (Fig. 3). Therefore, when airflow is ignored, the behaviour of an air-confined aquifer may be mistaken as that of a water-confined aquifer.

Change of hydraulic head fluctuation with horizontal distance

Figure 4 shows how the amplitudes of the hydraulic head fluctuation in the aquifer change with the distance from the coastline. The larger the ratio of k_U/k_L , the faster the amplitude attenuates landward. At the coastline, the amplitude of the hydraulic head for each case equals that of the tidal level, but at some inland location the amplitude with a small ratio of k_U/k_L is higher than that with a large ratio of k_U/k_L .

As discussed above, the increase in k_U/k_L reduces the air pressure fluctuation above the water table, which in turn weakens the impact of the air pressure on the water-table fluctuation. In other words, the water table will fluctuate more freely for large values of k_U/k_L . In this case, as the hydraulic head of the aquifer fluctuates, the variation of water volume in the aquifer increases so that the landward attenuation of the tide-induced head fluctuation becomes much faster (Fig. 4). Therefore, the local water-head fluctuation tends to be weak as the ratio of k_U/k_L becomes larger. In a water-confined aquifer, the diffusivity is calculated as the ratio of the hydraulic conductivity to the specific storage of the aquifer and is much greater than diffusivity in an air-unconfined aquifer. As a

result, the attenuation of the hydraulic head fluctuation with landward distance is much slower in a water-confined aquifer.

Vertical change of hydraulic head fluctuation in the saturated zone

Figure 5 shows how the amplitude of the hydraulic head fluctuation at a landward distance of 23 m changes with depth below the ground surface for different values of k_U/k_L with $k_L = 10^{-11} \text{ m}^2$. As discussed previously, the amplitude of the hydraulic head fluctuation decreases with the ratio of k_U/k_L at the same inland location. When the ratio of k_U/k_L is large, the tide-induced airflow is minor and the amplitudes of the hydraulic head fluctuations increase with depth (Fig. 5). Erskine (1991) observed a similar phenomenon in the field, i.e. that the deeper piezometers had smaller lags and larger tidal efficiencies. He thought the reason was that the pressure waves were more damped close to the phreatic surface since the storage relevant to this area is larger than the storage in the deeper aquifer where conditions are effectively confined. As the ratio of k_U/k_L decreases, airflow above the water table increases and the fluctuation of the phreatic surface is prohibited. Therefore, as shown in Fig. 5, the difference between the hydraulic head at different depths decreases with decrease of k_U/k_L . In the water-confined aquifer, the amplitudes of the hydraulic head at different depths are almost the same.

Figure 6 compares the temporal change of hydraulic head at three different depths in an air-unconfined aquifer without airflow (Fig. 6(a)) and in

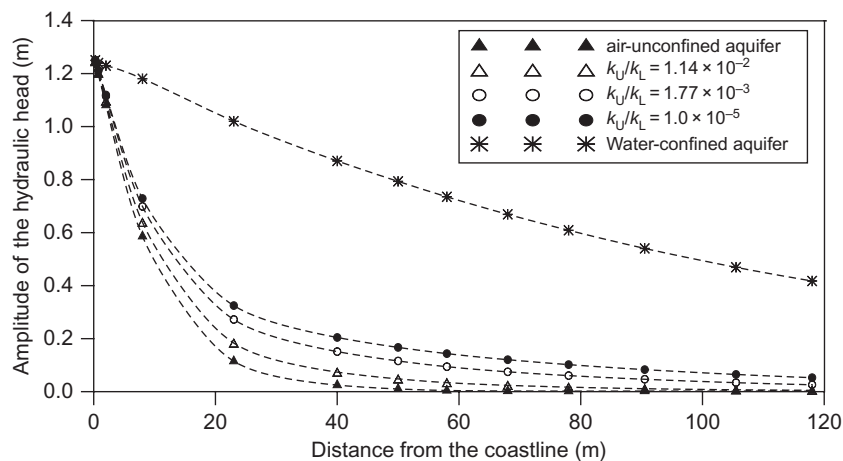


Fig. 4 Changes of the amplitudes of the hydraulic head in the middle of the aquifer (6.95 m b.m.s.l.) with distance from the coastline for different ratios of k_U/k_L with $k_L = 10^{-11} \text{ m}^2$.

Downloaded By: [University of Hong Kong] At: 02:39 24 April 2010

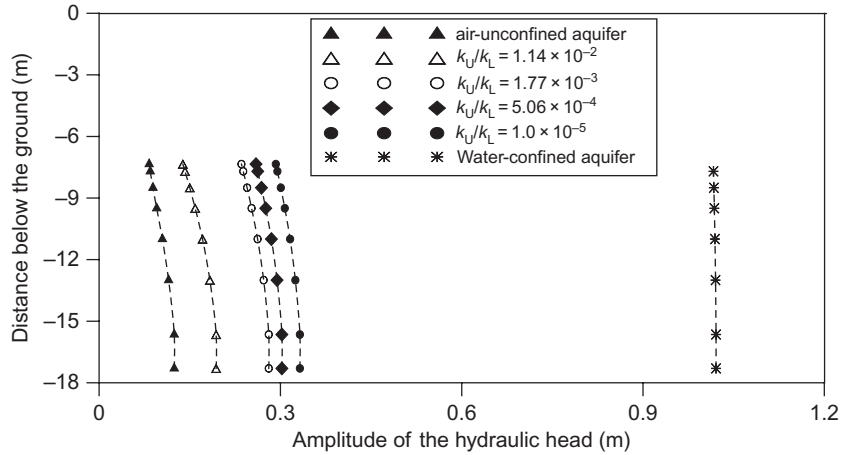


Fig. 5 Change of the amplitude of the hydraulic head fluctuation at a horizontal distance of 23 m from the coastline with depth below ground level for different ratios of k_U/k_L with $k_L = 10^{-11} \text{ m}^2$.

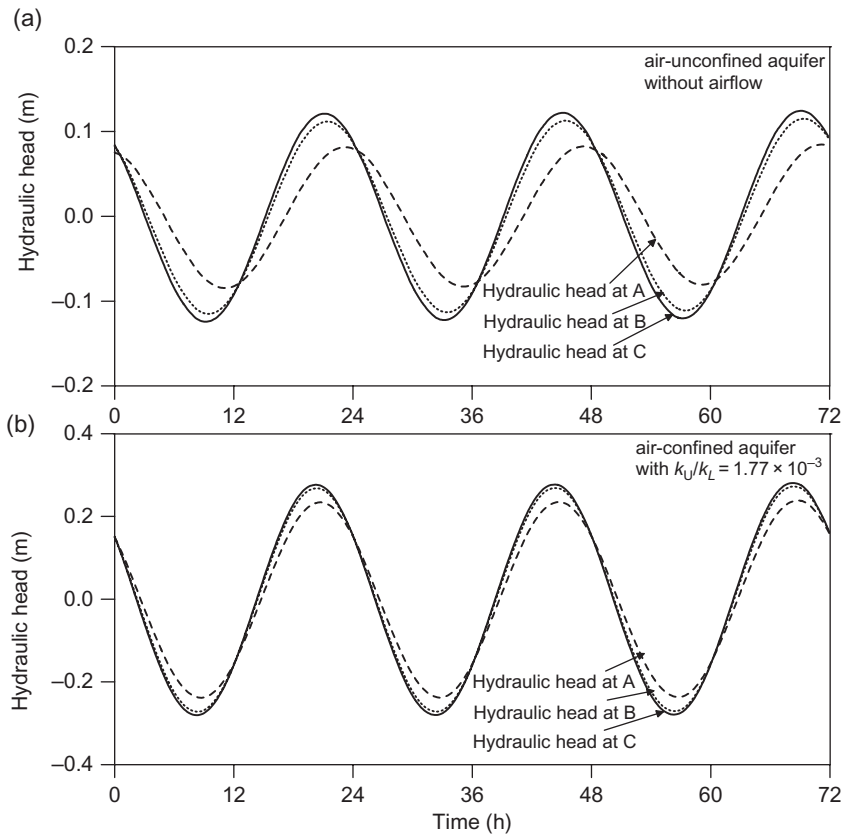


Fig. 6 Temporal change of hydraulic head at three observation points of different depths: (a) in an air-unconfined aquifer without airflow and (b) in an air-confined aquifer with $k_U/k_L = 1.77 \times 10^{-3}$. The observation points A, B and C (see Fig. 1 for locations) are at depths of 7.7 m (dashed curves), 13 m (dotted curves), and 17.3 m (solid curves) below the ground surface, respectively.

an air-confined aquifer with $k_U/k_L = 1.77 \times 10^{-3}$ (Fig. 6(b)). The amplitude increases with depth, and the hydraulic head fluctuation at small depth lags that at greater depth in the case without airflow (Fig. 6(a)).

This is because pressure waves are damped more significantly near the water table. The amplitudes of the hydraulic head fluctuations at three points (A, B and C) are 0.09, 0.12 and 0.13 m, respectively. In an

air-confined aquifer with $k_U/k_L = 1.77 \times 10^{-3}$ (Fig. 6(b)), the difference of the hydraulic head fluctuations at different depths decreases greatly due to impact of the airflow on the hydraulic head. The amplitudes at points A, B, and C increase to 0.24, 0.27 and 0.28 m, respectively, which are very close to one another. Also, the phase differences of the head fluctuations among these three points decrease greatly compared with those in an air-unconfined aquifer when airflow is negligible.

THE IMPACT OF AIRFLOW ON PARAMETER ESTIMATION

The analytical solution for the tide-induced hydraulic head fluctuation in water-confined aquifers for a straight coastline may be expressed as (Jacob, 1950):

$$H(x, t) = A \exp\left(-\sqrt{\frac{\omega S}{2T}}x\right) \times \cos(\omega t - \sqrt{\frac{\omega S}{2T}}x + c) \quad (10)$$

The sea tide is assumed sinusoidal and equal to $A \cos(\omega t + c)$. The variable $H(x, t)$ denotes the hydraulic head of the water-confined aquifer at inland position x and at time t as the datum is the mean sea level. The parameters A , ω and c are the amplitude, frequency and phase shift of the sea tide, respectively; S and T are the storativity [-] and transmissivity [$L^2 T^{-1}$] of the water-confined aquifer, respectively. Equation (10) shows that the amplitude of the groundwater-level fluctuation decreases exponentially with distance and the phase lag increases linearly.

Jacob's (1950) solution is frequently used to estimate the hydraulic parameters and discuss the groundwater regime of coastal water-confined aquifers. Equation (10) can also be applicable as a good approximation to water table fluctuations of an unconfined aquifer if the range of fluctuation is small compared with the saturated thickness (Erskine, 1991; Todd &

Mays, 2005). In most cases, equation (10) is utilized to estimate the aquifer diffusivity, D , i.e. the ratio of transmissivity to storativity (Freeze & Cherry, 1979). For an unconfined aquifer, the aquifer diffusivity can be approximated as the ratio of the transmissivity to the specific yield.

As discussed previously, the amplitude of the hydraulic head fluctuation increases due to the impact of airflow above the water table. Therefore, some errors may be induced if equation (10) is used for the parameter estimation in air-confined aquifers. The "true diffusivity" of the aquifer can be obtained by equation (10) with tidal data at point B in the air-unconfined aquifer without airflow. With $A_B = 0.11$ m at $x = 23$ m (Table 2), the hydraulic diffusivity, D , of the air-unconfined aquifer is calculated as 3.26×10^{-3} m²/s. Then the hydraulic diffusivity is estimated with tidal data at point B in air-confined aquifers. By comparing the "estimated" and "true" values of parameter D , one can see the parameter estimation errors caused by the airflow.

The true and estimated hydraulic diffusivities as well as their relative errors are listed in Table 3. The errors for the estimated values can be very great if the impact of airflow on hydraulic head fluctuation is neglected. In an air-confined aquifer with $k_U/k_L = 1.0 \times 10^{-5}$, the hydraulic diffusivity is overestimated by as much as 218%. The parameter estimation errors decrease as the ratio of k_U/k_L increases. This is because the impact of airflow on hydraulic head fluctuations becomes weaker as k_U/k_L increases. When $k_U/k_L = 1.12 \times 10^{-1}$, the diffusivity, D , is overestimated by only 8%.

CONCLUSIONS

The tide-induced hydraulic head fluctuation results in air pressure fluctuations above the water table, which in turn influences the hydraulic head fluctuation in the aquifer. In this paper, the impact of tide-induced airflow on hydraulic head fluctuation in a two-layered subsurface system was investigated using numerical

Table 3 Impact of airflow on parameter estimation when airflow is neglected.

k_U (m ²)	k_U/k_L	True diffusivity, D (m ² /s)	A_B (m)	Estimated diffusivity, D_e (m ² /s)	$(D_e - D)/D$ (%)
1.12×10^{-12}	1.12×10^{-1}	3.26×10^{-3}	0.12	3.52×10^{-3}	8
1.14×10^{-13}	1.14×10^{-2}	3.26×10^{-3}	0.18	5.13×10^{-3}	57
1.77×10^{-14}	1.77×10^{-3}	3.26×10^{-3}	0.27	8.20×10^{-3}	152
5.06×10^{-15}	5.06×10^{-4}	3.26×10^{-3}	0.29	9.02×10^{-3}	177
1.0×10^{-16}	1.0×10^{-5}	3.26×10^{-3}	0.32	1.04×10^{-2}	218

models. The system consists of upper and lower layers with permeabilities of k_U and k_L , respectively. The simulation results reveal that airflow has an impact on water level fluctuation in the aquifer when the ratio of k_U/k_L is low. In an air-confined aquifer, both the amplitude of the hydraulic head and the influence distance increase due to the impact of airflow. The local water-head fluctuation tends to increase as the ratio of k_U/k_L decreases. The fluctuations of the hydraulic head in air-confined aquifers tend to be similar to those in a water-confined aquifer. Thus the behaviour of an air-confined aquifer may be mistaken for that of a water-confined aquifer if airflow is neglected.

For a fixed distance from the coastline, the amplitude increases with the depth, and the hydraulic head fluctuation at small depth lags that at great depth. This is because the storage close to the water table is larger than that in the deeper aquifer so that the pressure waves at small depths are more damped. As the ratio of k_U/k_L decreases, the airflow becomes more significant, which prohibits the fluctuation of the water table. Thus the damping effect of the water table on transmission of the pressure waves becomes weak so that the differences of the hydraulic head fluctuations at different depths decrease.

In traditional studies on parameter estimation and groundwater regimes in coastal aquifers, airflow in the unsaturated zone is generally neglected, i.e. the air is treated as a passive bystander at constant pressure. However, as described in this paper, the airflow may be strong and have a significant impact on the aquifer response, which may lead to great errors in estimating hydraulic parameters when models that do not consider airflow are applied. In some cases, if airflow is neglected, the hydraulic diffusivity can be significantly overestimated. The parameter estimation errors increase as the ratio of k_U/k_L decreases.

In field situations, the water–land interface at the coastline may be more complex than that used in this study. Vandenbohede & Lebbe (2007) investigated the propagation of a tidal wave in a cross-section along the French–Belgian border perpendicular to the coast. In their study, there exists a sloping beach interacting with the tidally varying sea level. They concluded that the induced tidal wave in the aquifer was dependent on the position on the beach. Therefore, the impact of tide-induced airflow could be more complex in real field situations due to complicated boundary conditions.

Acknowledgements The study was supported by the Research Grants Council of the Hong Kong Special Administrative Region, China (HKU 7028/05P). TOUGH2 was run via the interface of PetraSim.

REFERENCES

- Ataie-Ashtiani, B., Volker, R. E. & Lockington, D. A. (2001) Tidal effects on groundwater dynamics in unconfined aquifers. *Hydrol. Processes* **15**, 655–669.
- Carr, P. A. (1969) Salt water intrusion in Prince Edward Island. *Can. J. Earth Sci.* **6**(1), 63–74.
- Carsel, R. F. & Parrish, R. S. (1988) Developing joint probability distributions of soil water retention characteristics. *Water Resour. Res.* **24**, 755–769.
- Carsel, R. F., Parrish, R. S., Jones, R. L., Hansen, J. L. & Lamb, R. L. (1988) Characterizing the uncertainty of pesticide movement in agricultural soils. *J. Contam. Hydrol.* **2**(2), 111–124.
- Chan, S. Y. & Mohson, M. F. N. (1992) Simulation of tidal effects on contaminant transport in porous media. *Ground Water* **30**(1), 78–86.
- Corey, A. T. (1954) The interrelation between gas and oil relative permeabilities. *Producers Monthly* **19**, 38–41.
- Elberling, B., Larsen, F., Christensen, S. & Postma, D. (1998) Gas transport in a confined unsaturated zone during atmospheric pressure cycles. *Water Resour. Res.* **34**, 2855–2862.
- Erskine, A. D. (1991) The effect of tidal fluctuation on a coastal aquifer in the UK. *Ground Water* **29**(4), 556–562.
- Freeze, R. A. & Cherry, J. A. (1979) *Groundwater*. Prentice-Hall, Englewood Cliffs, New Jersey, USA.
- Guo, H. P. & Jiao, J. J. (2008) Numerical study of airflow in the unsaturated zone induced by sea tides. *Water Resour. Res.* **44**, W06402. doi:10.1029/2007WR006532.
- Guo, H. P., Jiao, J. J. & Weeks, E. P. (2008) Rain-induced subsurface airflow and Lisse effect. *Water Resour. Res.* **44**. doi:10.1029/2007WR006294.
- Jacob, C. E. (1950) Flow of groundwater. In: *Engineering Hydraulics* (ed. by H. Rouse), 321–386. John Wiley, New York, USA.
- Jiao, J. J. & Li, H. L. (2004) Breathing of coastal vadose zone induced by sea level fluctuations. *Geophys. Res. Lett.* **31**, L11502. doi:10.1029/2004GL019572.
- Jiao, J. J. & Tang, Z. H. (1999) An analytical solution of groundwater response to tidal fluctuation in a leaky confined aquifer. *Water Resour. Res.* **35**, 747–751.
- Leung, W. K., Li, C. H. & Pickles, A. R. (2007) Heaving of airfield pavement at Hong Kong International Airport. *Proc. 2007 FAA Worldwide Airport Technology Transfer Conference*, Atlantic City, USA.
- Li, H. L., & Jiao, J. J. (2005) One-dimensional airflow in unsaturated zone induced by periodic water table fluctuation. *Water Resour. Res.* **41**, W04007. doi:10.1029/2004WR003916.
- Li, H., Li, L. & Lockington, D. (2005) Aeration for plant root respiration in a tidal marsh. *Water Resour. Res.* **41**, W06023. doi:10.1029/2004WR003759.
- Li, L., Barry, D. A. & Pattiaratchi, C. B. (1996) Modeling coastal ground-water response to beach dewatering. *J. Waterway, Port, Coastal, and Ocean Engng* **122**(6), 273–280.
- Mualem, Y. (1976) New model for predicting hydraulic conductivity of unsaturated porous-media. *Water Resour. Res.* **12**, 513–522.
- Pandit, A., Ei-Khazen, C. C. & Sivaramapillai, S. P. (1991) Estimation of hydraulic conductivity values in a coastal aquifer. *Ground Water* **29**(2), 175–180.

- Pontin, J. M. A. (1986) Prediction of groundwater pressures and uplift below excavation in tidal limits. In: *Groundwater in Engineering Geology* (ed. by J. C. Cripps, F. G. Bell & M. G. Culshaw), 353–366. Geological Society of London, UK.
- Pruess, K., Oldenburg, C. & Moridis, G. (1999) *TOUGH2 User's Guide, Version 2.0*. Earth Sci. Div., Lawrence Berkeley Natl. Lab., Univ. of California, Berkeley, USA.
- Robinson, M. A. & Gallagher, D. L. (1999) A model of ground water discharge from an unconfined coastal aquifer. *Ground Water* **37**(1), 80–87.
- Shan, C. (1995) Analytical solutions for determining vertical air permeability in unsaturated soils. *Water Resour. Res.* **31**, 2193–2200.
- Sheahan, N. T. (1977) Injection/extraction well system – a unique seawater intrusion barrier. *Ground Water* **15**(1), 32–49.
- Todd, D. K. & Mays, L. W. (2005) *Groundwater Hydrology* (Third edn), 299–302. John Wiley, Hoboken, New Jersey, USA.
- van Genuchten, M. T. (1980) A closed-form equation for predicting the hydraulic conductivity of unsaturated soils. *Soil Sci. Soc. Am. J.* **44**, 892–898.
- Vandenbohede, A. & Lebbe, L. (2007) Effects of tides on a sloping shore: groundwater dynamics and propagation of the tidal wave. *Hydrogeol. J.* **15**, 645–658.
- Weeks, E. P. (2002) The Lisse effect revisited. *Ground Water* **40**, 652–656.